PLAT-O #2 at FloWave: A tank-scale validation of ProteusDS at modelling the response of a tidal device to currents (Part 2)

Ilie Bivol [#1], Penny Jeffcoate [*2], Lars Johanning [‘3], Ryan Nicoll [~4], Jeffrey Steynor [^5], Vengatesan Venugopal [+6]

[#1] *IDCORE, University of Edinburgh, Scotland;* I.Bivol@ed.ac.uk
[*2] *Sustainable Marine Energy Ltd, Scotland;* penny.jeffcoate@sustainablemarine.com
[‘3] *University of Exeter, England;* L.Johanning@exeter.ac.uk
[~4] *Dynamic Systems Analysis, Canada;* ryan@dsa-ltd.ca
[^5] *FloWave Test Facility, Scotland;* Jeff.Steynor@ed.ac.uk
[+6] *University of Edinburgh, Scotland;* V.Venugopal@ed.ac.uk

Abstract— **PLAT-O #2 is a subsea floating tidal energy generator. A scaled-down physical model of this device was tested at FloWave in steady axial currents of up to 6.2 m/s (full-scale). The platform's motion and mooring tensions were measured to validate a tank-scale numerical model in ProteusDS. In currents above 3.5 m/s (full-scale) the platform with turbines was observed to squat in an arc motion about the upstream lines to a stable lower depth, to balance the forces of drag, thrust, net buoyancy and lift.**

Hydrodynamic characteristics of the platform are derived from these experiments to aid the model calibration. A significant downward lift towards the bed is observed when the platform (with turbines) pitches bow-up to the flow. The downward lift acts to lower upstream line tensions but encourages the squatting motion. The platform's drag coefficient is observed to reduce with the tank flow, by up to 15% at 1.24 m/s (critical, Re ≈ 2×10^5) relative to the value at 0.40 m/s (sub-critical, Re ≈ 5×10^4).

Representing the downward lift and the Reynolds-dependent drag in the numerical model resulted in accurate predictions of mooring tensions (< 5%) and motion (< 1 standard deviation). Further work includes: a wave-current validation, the flume-testing of the platform for more comprehensive lift and drag characteristics; the optimisation of the mooring geometry to control squatting, and CFD studies to predict lift in the sea.

***Keywords*— Floating Tidal Generator; ProteusDS Dynamic Analysis; Tank Testing; Lift; Morison method**

I. INTRODUCTION

Floating tidal generators can power island communities with economical, renewable and predictable electricity. Subsea floating devices, such as Sustainable Marine Energy's PLAT-O range [1], enable optimization of yield, survivability and O&M costs. The first full-scale prototype (#1) is shown in Figure 1. The PLAT-O #2 (Fig. 2), the subject of this study, is the next-generation concept, hosting four SCHOTTEL Hydro SIT250 62 kW turbines [2]. The device is moored in tension, mid-depth, by a bridled system of four primary lines and eight secondary lines. For more details see previous published work in [3][4].

Tidal generation sites are dynamic environments (e.g. time and spatially-varying) with turbulent currents of distinct vertical profiles. Understanding PLAT-O #2's response to environmental conditions in terms of platform motion and mooring tensions is essential for designing a safe, cost-effective and durable device. To reduce the risk of catastrophic failure, the mooring specification must be informed by numerical models using robust tools that have been validated against tank experiments to sufficient accuracy. Engineering standards and recommended practices that can be applied to the permanent mooring of floating tidal devices include [5]-[7].

A 1:17 scale physical model of PLAT-O #2 (Fig. 3) was tested at the Edinburgh University's FloWave facility [8] for currents expected at the EMEC tidal site [9]. The platform motion, mooring tensions and current velocity were measured in the tank to validate numerical models in ProteusDS.

ProteusDS is a time-domain tool for modelling the dynamic response of offshore structures [10]. It is a semi-empirical multibody dynamics model that includes an extended Morison method for hydrodynamic loads and a finite-element model for mooring-structure loads and dynamics. ProteusDS provides accurate and computationally efficient results for early concept development. Case studies of ProteusDS being used for the dynamic analysis of floating tidal devices include [4][11].

Previously, the PLAT-O #2 tank set-up was simulated at tank-scale in ProteusDS. A 'current-only' validation study [4] resulted in comparable platform motion but overestimated mooring tensions. A significant platform lift and Reynolds-dependent drag, unaccounted for in [4], were suspected. This paper presents an improved methodology (to that in [4]) that quantifies the lift, drag and thrust forces in the tank and represents these in the numerical model for more accurate predictions of device motion and mooring tensions.

Fig. 1 PLAT-O #1 full-scale prototype [1]

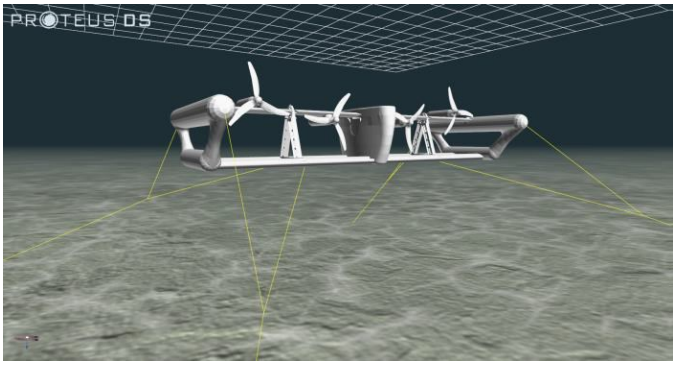

Fig. 2 A 3D visualisation of PLAT-O #2 platform and mooring lines [3]

II. METHODOLOGY

This section covers the test subject, the forces at work, the experimental and numerical set-ups, and the path from tank data processing to ProteusDS model validation.

A. Environmental forces

The PLAT-O #2 device hosts four turbines on a floating platform that is moored in tension and in the middle of the water column by a bridled spread of four anchors, four primary and eight secondary lines (refer to Fig. 2). The platform is a streamlined assembly of pontoons, connected at the keel by near-elliptical beams in tandem and near the top by hydrofoil beams supporting the turbines. The turbines are mounted on the hydrofoil beams such that the rotors are downstream of the foil. The hydrofoil beams are free to rotate and level with flow to serve as a passive flipping mechanism when the tide turns and are not intended to provide lift, but only to reduce the drag and the disturbed flow into the downstream rotors [3][4].

The forces acting on the platform in currents and no waves are drag (F_D), lift (F_L), turbine thrust (F_T) and net buoyancy (F_{NB}), as shown in Figure 4. The platform has a mass-inertia (own mass and added mass); however, at high flow speeds, and thus Reynolds numbers, inertial effects are negligible compared to viscous effects. Each platform force (e.g. weight) acts about an individual centre (e.g. Centre of Gravity). The mooring system restrains all platform loads in tension (e.g. $T_{U,\,D}$) and about a centre of effort. The device reaches equilibrium when all forces and moments are balanced. In still water, pre-tension is kept in the lines by the net buoyancy, which is constant for a fully submerged platform.

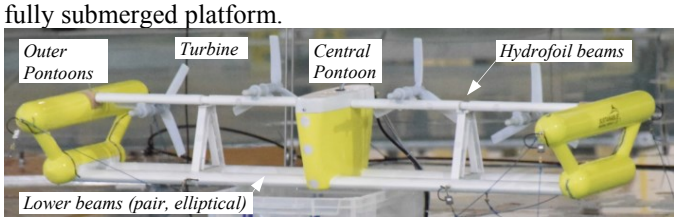

Fig. 3 PLAT-O #2 physical model faced bow-side

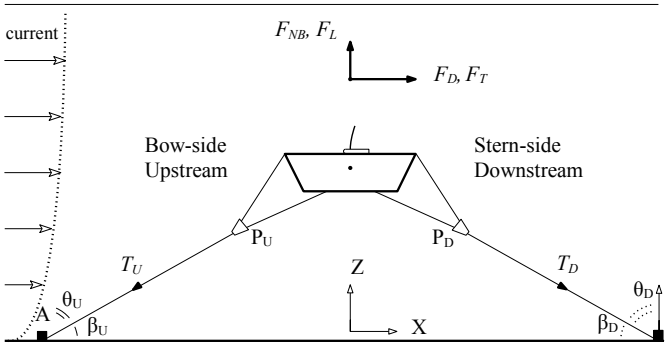

Fig. 4 PLAT-O #2 environment and main forces (2D side-view)

B. Tank Testing

The 1:17 scale model of PLAT-O #2 (Fig. 3) was tank-tested with and without turbines in currents of up to 1.17 m/s (4.8 full-scale) and 1.50 m/s (6.2 full-scale), respectively. This allows the impact of turbine thrust on the device response to be isolated.

The turbines are geometrically-scaled in diameter (4 m at full-scale), free-wheeling (no torque) and with a modified blade profile for thrust similitude [3]. A mooring member in the tank consists of three ropes, a split plate, a spring and a load-cell, as shown in Figure 5. The springs, used to achieve stiffness similitude [3], are located at the anchors.

The tank is instrumented to record the following items: flow velocity (3D) using a Nortek Vectrino velocimeter, device motion (6DOF) using a Qualysis motion capture system and an accelerometer, and mooring loads using National Instruments cells. The Vectrino is fixed 0.5 m above and 1 m downstream from the top of the central pontoon in still water (Fig. 5).

Statistics of the tested flows – mean speed (v), standard deviation of speed, turbulence intensity (TI) and mean directions (dir) – for each configuration are calculated from the Vectrino records and summarised in Table I. Generally, the standard deviation of flow speed increases in faster currents, describing an increasing turbulence. The ranges of recorded turbulence intensities are 6 – 8% (no turbines) and 15 – 35% (with turbines). The flow characteristics during the 0.56 m/s test with turbines stand out from the rest with the highest standard deviation of 0.20 and TI of 35%, because of unsettled turbulence in the tank prior to the experiment. The Vectrino may be encountering additional turbulence due to its close proximity to the platform and turbines. The flow directions are very close to axial (< 2°). The measured vertical Z-components of current are negligible (< 0.03 m/s).

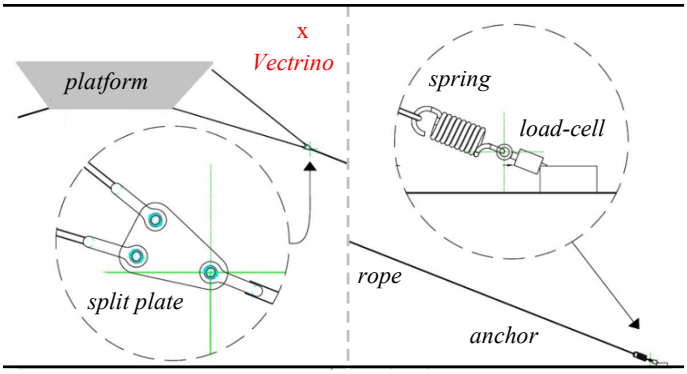

Fig. 5 Tank mooring make-up and instrumentation (not to scale)

TABLE I: TESTED CURRENTS AND DEVICE CONFIGURATIONS

Set - up	Tank flow characteristics						
No turbines	v mean	m/s	0.40	0.69	0.95	1.24	1.50
	v std	m/s	0.03	0.05	0.06	0.07	0.11
	TI mean	%	8	8	6	6	8
	dir mean	deg	0.4	0.5	0.6	0.7	1.1
With turbines	v mean	m/s	0.37	0.56	0.60	0.84	1.17
	v std	m/s	0.07	0.20	0.12	0.15	0.18
	TI mean	%	19	35	20	17	15
	dir mean	deg	1.8	1.2	0.3	2.4	1.0

C. Experimental Platform Drag and Lift Derivation

Device position and mooring line loads are essential performance metrics for concept design validation. The drag, lift and thrust are the main contributors to these and should be represented accurately in the numerical model. These are experimentally derived from tank data and are used to calibrate numerical model inputs.

The platform drag and lift characteristics in the tank are derived by projecting primary line tensions in the global axes (X and Z, in-line and normal to flow, Fig. 4) and solving the free-body-diagram for equilibrium (Eq. 1 and 2). Line tensions (T) are projected about the X and Z axes by the corresponding β and θ angles. The subscripts U and D refer to upstream and downstream elements. The projection is about the absolute 3D angle between the line vector (e.g. $\overrightarrow{AP_U}$ for one upstream line) and the axis unit vector (e.g. $\vec{Z}$ for the Z-axis) found by the dot product (Eq. 3). Each line vector is obtained from the locations of its split plate (P, recorded or derived from Qualysis) and its anchor (A, as per set-up). The split plate locations are recorded by Qualysis. When motion capture cameras are unable to view the position markers, the plate positions are estimated from the overall platform position. This is done by fixing the platform position in ProteusDS to that recorded in the tank and outputting the locations of the bridle. The net buoyancy is calculated from measurements in still water.

$$\textbf{Eq. 1} \quad F_D = 2\,[T_U\,cos(\beta_U) - T_D\,cos(\beta_D)]$$

$$\textbf{Eq. 2} \quad F_L = 2\,[T_U\,cos(\theta_U) + T_D\,cos(\theta_D)] - F_{NB}$$

$$\textbf{Eq. 3} \quad cos(\theta_U) = \frac{\overrightarrow{AP_U}\cdot\vec{Z}}{|\overrightarrow{AP_U}|\,|\vec{Z}|}$$

Drag and lift coefficients are calculated for the whole platform (Eq. 4 and 5), where v is the measured mean current speed and ρ is the water density at 1000 kg/m^3. The reference area (A) is 0.217 m^2, assumed to be the mean of XY plane cross-sections of each shape in the assembly.

$$\textbf{Eq. 4} \quad C_D = \frac{F_D}{0.5\rho A v^2}$$

$$\textbf{Eq. 5} \quad C_L = \frac{F_L}{0.5\rho A v^2}$$

In flows higher than 3.5 m/s at full-scale, the downstream lines slacken and the platform squats gradually to a stable position along the loci of the upstream mooring lines [3][4]. During squatting, the upstream mooring angles (β_U) reduce to balance components of mooring tensions in the X and Z axes (Fig. 4). The vertical Z-component reacts the net buoyancy and lift forces. The horizontal X-component reacts the drag (and thrust) forces (with turbines).

Regarding experimental data processing, the usable test durations are typically 60 s after periods of current ramp-up are removed. Outliers and noise are filtered by a low-pass Fast Fourier transform. Tensions and motions are recorded at 256 and 128 Hz, respectively, and filtered to 16 Hz. Experimental results are then directly compared with simulations at tank-scale in ProteusDS.

D. ProteusDS Modelling

ProteusDS is a multibody time domain dynamics model that includes a Morison method approach for hydrodynamic loading (drag, inertia) from prescribed metocean conditions and a finite element model [12] for mooring structure loads and dynamics. Turbines are modelled as point forces and moments.

The tank's vertical profile follows a 1/15th power law [13]; more uniform than that of a typical tidal site (1/7th or 1/10th); modelled as uniform in this study. The modelled currents are the mean measured by the Vectrino, steady, perfectly axial and without turbulence at this stage.

The Morison method estimates current loads on bodies as the linear addition of drag and inertia [14]-[16]. The semi-empirical formula requires hydrodynamic coefficients of drag (C_D) and inertia (C_M) for the subject structure to be derived experimentally; however, tables of a wide range of cross-sections, shapes and test conditions are available in literature [15]-[17] and standards [14]. The Morison method does not resolve wakes from fluid-structure interaction; therefore, any shielding or reduced in-flows on structures placed downstream of another are not captured. The hydrodynamic parameters are a function of geometry, flow regime (Re) and surface roughness (k/D) [15][16]. Drag coefficients for cylinders of various roughness values in steady flow depending on the Reynolds flow regime [14] are given in Figure 6. For a cylinder with a k/D of 1×10^{-5} (highlighted in Fig. 6), the C_D curve drops from 1.2 to 0.3 between $Re \approx 2\times10^4$ (sub-critical) and $Re \approx 2\times10^5$ (critical), and then recovers to 0.7 at $Re > 10^6$ (post-critical). The critical Re value is specific to a geometry and roughness.

The PLAT-O #2 physical model has a composite surface of a roughness k/D estimated between 5×10^{-5} and 5×10^{-6} [14]. The flow regime across the platform ranges from $Re \approx 5\times10^4$ at 0.40 m/s to $Re \approx 3\times10^5$ at 1.50 m/s. The tank-derived platform drag curve confirms a critical flow regime and significant reductions in C_D in the higher Reynolds numbers. The characteristic length is taken as the mean longitudinal value of all assembly geometries. A more in-depth description of the Morison method and the ProteusDS process (inputs, methods and capabilities) as applied to this study is given in [4].

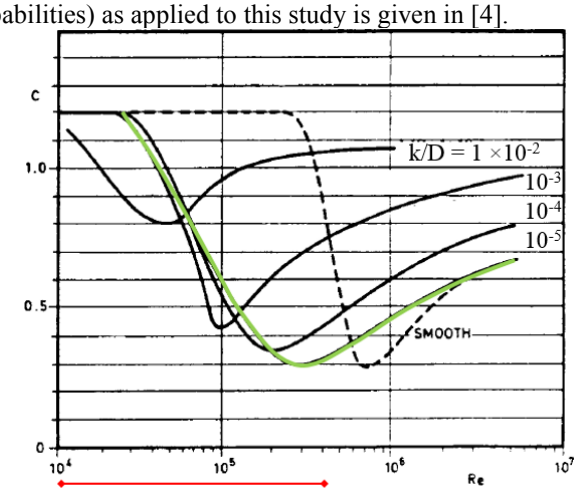

Fig. 6 Drag coeff. of a cylinder in steady flow as a function of Reynolds (Re) and surface roughness (k/D) [14]. Experimental regime of this study in red

The PLAT-O #2 geometry is modelled as a 3D rigid assembly of generic (e.g. cuboid) and custom bodies (Fig. 7). The mooring spread - anchors, springs, lines, bridles and yokes points (Fig. 5) – is modelled to match the static platform set-up and assumed symmetric (i.e. equal line lengths). The line pre-tension is matched by adjusting mass to 130% of the real value. This is because the platform volume, and consequently the buoyancy, is overestimated from representing its curved and streamlined features (e.g. central pontoon) as rough generic shapes (e.g. cuboid). The platform volume, inertia and drag can be represented more accurately in ProteusDS with custom streamlined shapes. This level of detail has not been implemented at this stage, apart from the elliptical lower beams.

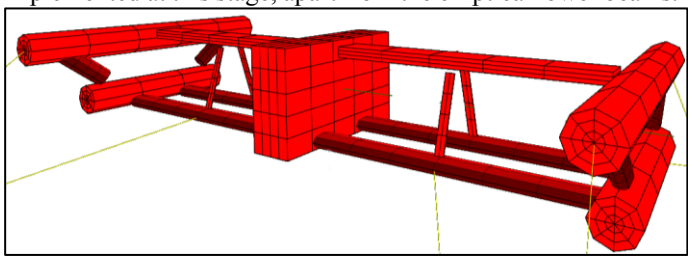

Fig. 7 PLAT-O #2 platform as an assembly of geometries in ProteusDS

E. Numerical Model Validation

To obtain accurate model outputs, all of the main forces in the tank must be accurately represented through the inputs; provided the tool is robust and fit for the specific application. It is important to be aware of the tool limitations (e.g. unresolved wake regions and shielding) and modelling assumptions (e.g. the drag on the communication cable and on the split plates is assumed to be negligible).

The tank data provides a valuable description of the platform drag, lift and thrust characteristics depending on its position and the inflow velocity. Hydrodynamic coefficients (C_D, C_M) for generic geometries and flow regimes are also available in literature. Comparing the two sources of information helps to understand the behaviours in the tank and to calibrate the model.

The modelling process is summarised below as:

1) The platform geometry, static position, pre-tension and mooring spread are replicated in the numerical model.
2) Drag coefficients are prescribed for each shape, initially from literature (as in [4]) and then calibrated to match the platform drag in the tank during the sub-critical 0.40 m/s test. For the calibration, the platform pitch in the model is the same as in the tank. The drag on the downstream lower beams is assumed to be 40% of that on the upstream beams, due to flow shielding [18]. These C_D values (calibrated to the sub-critical test) are kept constant in the higher flows.
3) Drag coefficients are reduced to account for the Reynolds dependency as the flow regime approaches critical. The reduction percentages come from tank data.
4) The platform lift is modelled via the hydrofoil feature in ProteusDS with inputs of force and moments for given angles of attack (or pitch) and assumed to act along the front lower beams. The lift force is as tank-derived and the moment is adjusted until the platform pitch is matched.
5) The thrust coefficient is calibrated from comparison of tests with and without turbines at the same current.

To investigate the impacts of Reynolds-dependent drag, lift and calibrated thrust on the validation agreement, the three forces have been modelled (steps 3, 4 and 5) in two selected test cases. The Reynolds-dependent drag and the lift are modelled (steps 3 and 4) for the 1.24 m/s test without turbines, when the platform squats. The lift is modelled (step 4) and the thrust is calibrated (step 5) for the 0.37 m/s test with turbines.

To accurately model platform drag and lift, it is essential that the modelled pitch matches the measured. For modelling platform drag, the objective is to represent the force as well as the centre, which affects the platform pitch. Drag coefficients are specified for each geometric component in the structure, so it is a challenge to distribute these based on the tank-derived drag for the whole assembly, and also account for flow shielding (e.g. reduced inflow on the downstream lower beams). For the drag calibration (steps 2 and 3), the initial C_D values from literature are all scaled up or down (keeping their relative proportions) until the modelled drag for the whole assembly matches the tank drag.

The lift also affects the platform pitch. The exact centre of lift is unknown at this stage. It is difficult to distinguish the individual contribution of drag and lift to platform pitch from the tank data. For that reason, a lift moment is added to correct the modelled pitch to that measured in the tank.

III. RESULTS

A. Empirical hydrodynamic characteristics

The device drag, thrust and lift forces are experimentally derived from primary tensions and split plate positions recorded during steady flow tests with and without turbines. The forces are normalized against the pre-tension in one primary line (T_0).

In terms of device loads in-line with flow, the thrust from operating turbines dominates platform drag, when comparing tests with and without turbines (Fig. 8).

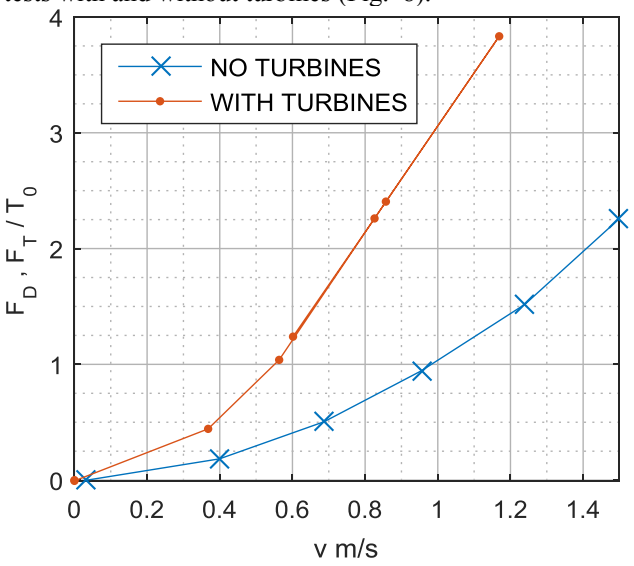

Fig. 8 Platform drag and thrust (forces in-line with flow) with mean flow

The platform drag coefficient drops as the inflow speed and the Reynolds numbers increase (Fig. 9). This is as anticipated from similar trends observed in cylinders (Fig. 7). The critical flow regime for the platform is $Re \approx 2\times10^5$ at 1.24 m/s, where the C_D is 0.33, which is 15% less than the sub-critical value of 0.38 at $Re \approx 5\times10^4$ and 0.40 m/s.

The tank-derived platform drag is used to calibrate C_D values in the numerical model. The tank drag curve is compared with modelling outputs from two iterations in Figure 10. The 'upper-bound' curve results from the conservative inputs used in the previous study [4] informed by literature only. The 'subcritical fit' curve is of this study, where the C_D values (from literature) are calibrated against the tank-derived drag at the subcritical 0.40 m/s test and are kept constant in the higher flows (and Reynolds numbers). The modelled drag is output from simulations with the platform pitch fixed to the real tank value. Deriving the experimental drag curve and using it as a baseline enables more accurate modelling of drag. The 'subcritical fit' iteration still slightly overestimates drag in higher currents because the reduction in C_D values due to the Reynolds regime is not accounted for in this step.

The tank-derived platform lift force as a function of pitch (or angle of attack) is presented in Figure 11. The platform pitches bow-up (or positive) with turbines in normal operation. In the absence of a thrust moment, the platform pitches bow-down (or negative). The platform is subject to significant lift as it pitches bow-up or bow-down in axial flows. The lift force is negative and it acts towards the bed (i.e. in the opposite direction to that initially assumed in Fig. 4). With turbines, the platform pitches bow-up and experiences a maximum downward lift of -0.45 at 3°. As the pitch increases past 4° in the higher flows the negative lift reduces (Fig. 12), which is a sign of stalling and the onset of uplift. Without turbines, the maximum lift is -0.7 when the platform pitches -3° (bow down) in 1.5 m/s flow (the strongest and most turbulent tested, equivalent to 6 m/s).

The platform lift coefficient as function of pitch is shown in Figure 12. The lift acts sharply with pitch, as indicated by the steep slopes at low angles of attack. There is some scatter in C_L values at very small pitch angles (0 ± 2°) that occur in the low speeds (0 – 0.6 m/s tank). This could be because of complex flow interactions and larger uncertainties in the measurements (relative to the mean value) in lower flow speeds. The C_L trends are more distinguishable at wider pitch angles with linear slopes observed for positive and negative directions (Fig. 12).

The next section presents the measured motion and mooring tensions in the range of tested flows, with and without turbines. The tank response is compared with concurrent outputs from simulations with and without the improvement of added lift, Reynolds-drag and calibrated thrust.

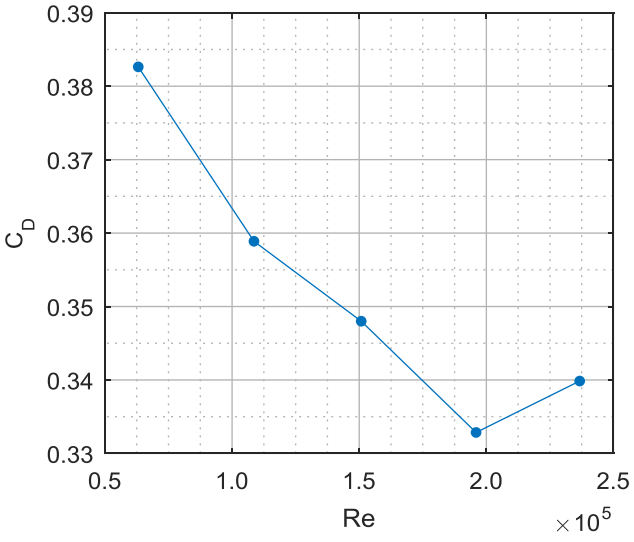

Fig. 9 Platform drag coefficients in the range of tested flow regimes

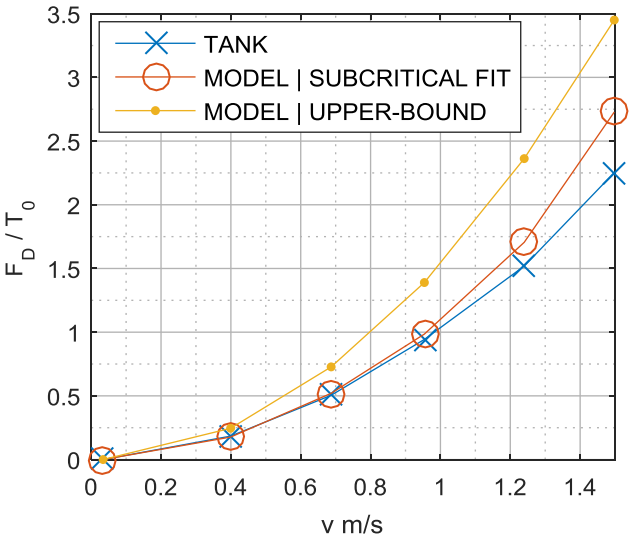

Fig. 10 Replicating tank-derived platform drag in the numerical model

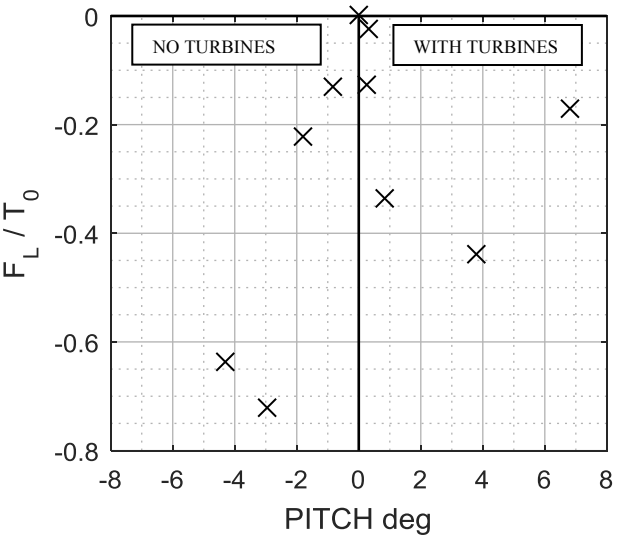

Fig. 11 Platform lift force (tank-derived) as a function of pitch (angle of attack)

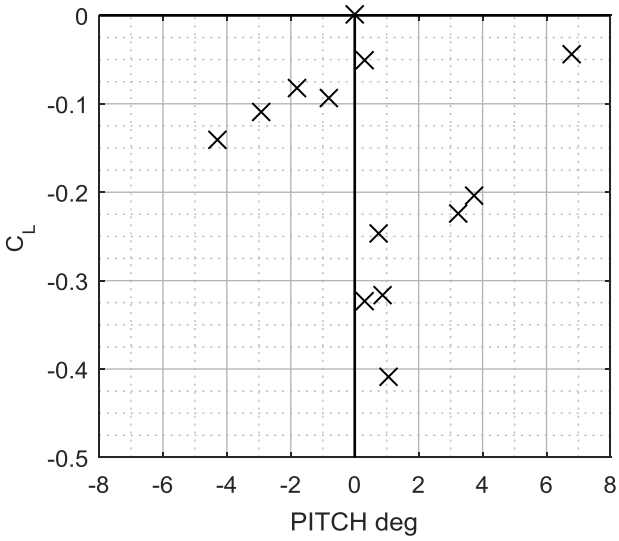

Fig. 12 Platform lift coefficient (tank-derived) with pitch (mean measured)

B. Device response in currents-only

Translational motion statistics are normalized against rotor diameter to give non-dimensional results. For the platform without turbines, the measured and modelled motions with flow are compared in Figure 13. The arc trends in surge and heave illustrate the platform squatting – forward with current and to a lower depth - in currents higher than 1.2 m/s (4.9 full-scale). When comparing agreement in surge and heave motion at 1.2 m/s (Fig. 13), the improved numerical model with lift and Reynolds-dependent drag, captures the squatting more accurately (within one standard deviation), than in the previous iteration. In the rest of the flow cases, the lift and Reynolds-dependent drag are not modelled in, which results in the squatting being underestimated. Therefore, the downward lift encourages the squatting and must be represented in the numerical model for improved motion validation.

The platform without turbines pitches bow-down or negative with the flow, to balance moments of platform loads (drag and lift) and mooring tensions about the transverse axis (Y-axis). The numerical model without lift underestimates the pitch, increasingly so with current (Fig. 13), because the unaccounted lift force, and consequently moment, increases with bow-down pitch (Fig. 11). In the numerical model with lift, the modelled pitch is corrected to match the tank, as shown in Figure 13, by calibrating the lift moment as described in the modelling method. The range of measured motions, e.g. min and max, increases with current due to a rise in turbulence, the increased compliance with squatting and the overcoming of buoyancy. The growing turbulence with flow speed is reflected by a rise in standard deviation of measured flow (refer to Table I). The numerical model does not capture the fluctuations in motion because the flow turbulence is not modelled at this stage.

Mooring tensions statistics are normalised against the average pre-tension in a primary line (T_0). In the tank, the load share between upstream lines is not even due to turbulence and a slightly asymmetric spread (e.g. line clamp slippage). For comparison, the measured loads are added and averaged.

For tests without turbines, the measured and modelled tension statistics for upstream and downstream lines are plotted against the current speed in Figure 14. The downstream lines start with a similar pre-tension to the upstream lines. As the flow increases, the downstream tension (in red, Fig. 14) is released with squatting and the recorded is just the line drag. The measured upstream line loads (in black, Fig. 14) generally increase with flow, with the exception at 1.2 m/s (when the platform starts squatting). The upstream line loads from the numerical model without lift (in red crosses, Fig. 14) increase quadratically with flow and are overestimations, increasingly so with current. Modelling with lift at 1.2 m/s, as oppose to no lift, captures more accurately the dip in tensions, as indicated by the green mark in Figure 14. This is because the downward lift counteracts pre-tension to lower upstream line tensions.

For the platform with turbines, the measured and modelled motions are compared in Figure 16. The additional thrust force causes the platform to squat at a lower current of 0.84 m/s (3.5 full-scale) than without turbines. The turbines cause the platform to have a positive bow-up pitch with flow, which is in the opposite direction and of a wider angle compared to cases without turbines. When comparing the measured heave and surge in Figures 13 and 16, the device squats deeper with turbines than without at the same current (e.g. 1.2 m/s). This is due to the turbines adding thrust and also causing larger pitch angles, and consequently platform drag.

Similar to cases without turbines (Fig. 13), the numerical model with turbines and no lift underestimates the squatting (Fig. 16). The downward lift has not been modelled for a squatting case with turbines on, but its inclusion is expected to improve, as in cases without turbines, the motion validation.

For tests with turbines, the measured and modelled tension statistics for upstream and downstream lines are plotted against mean current in Figure 17. The upstream tank tensions follow a clear quadratic trend with flow as expected in an environment dominated by drag and thrust. The modelled upstream line tensions without lift are overestimated and outside the measured range. In the modelled case at 0.37 m/s with lift and calibrated thrust, the tension validation is improved to within 3%. The calibrated thrust value is 90% of the ideal, providing some certainty that the tank turbines perform close to intended design.

The modelling error values in the upstream tensions for both turbine cases and modelling iterations are given in Figure 15. The numerical model with constant sub-critical drag coefficients, and no lift, overestimates upstream loads by up to 20% (with turbines) and 30% (without turbines), as shown by red markers in Figure 15. If the drag coefficients are calibrated for Reynolds effects, and the lift is modelled in, the line tensions are comparable, within less than 5% in both turbine cases, as shown by the green markers in Figure 15. The results are consolidated and discussed in more detail in the next section.

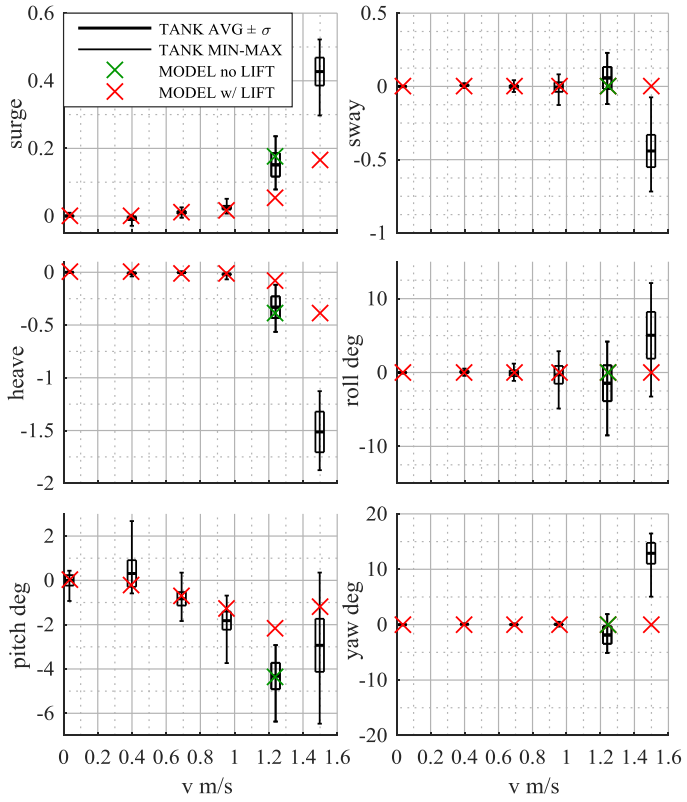

Fig. 13 Platform without turbines - motion validation

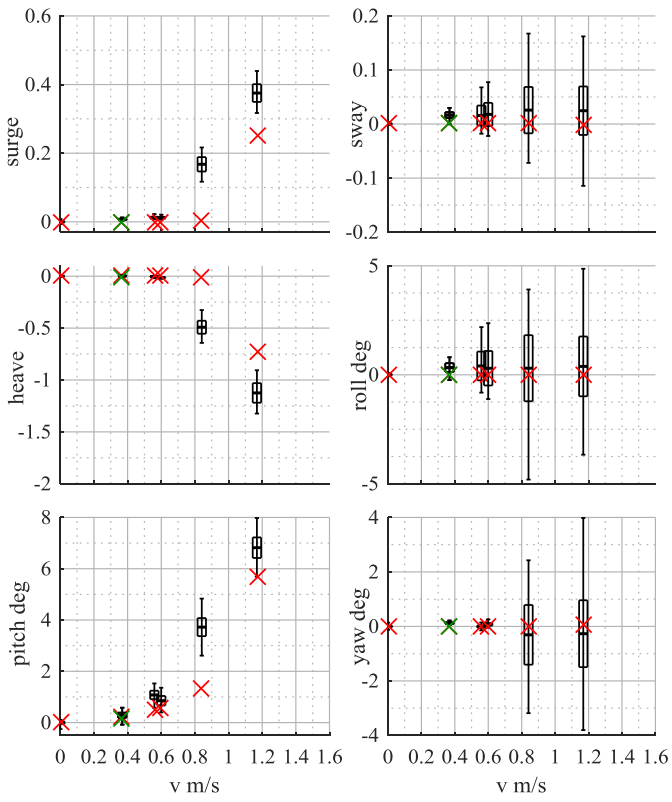

Fig. 16 Platform with turbines - motion validation

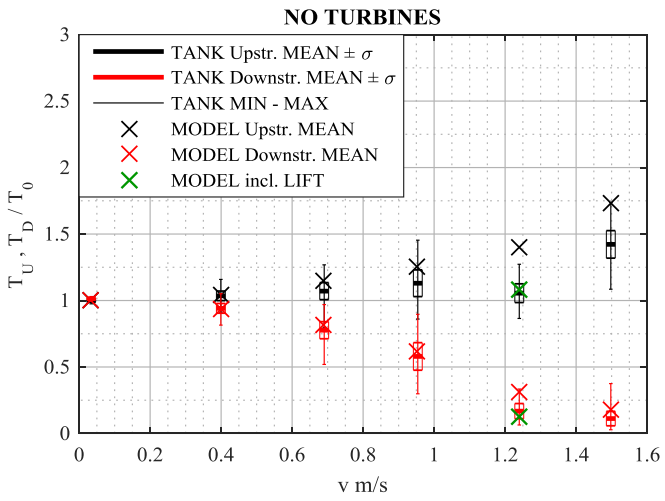

Fig. 14 Platform without turbines – mooring tensions validation

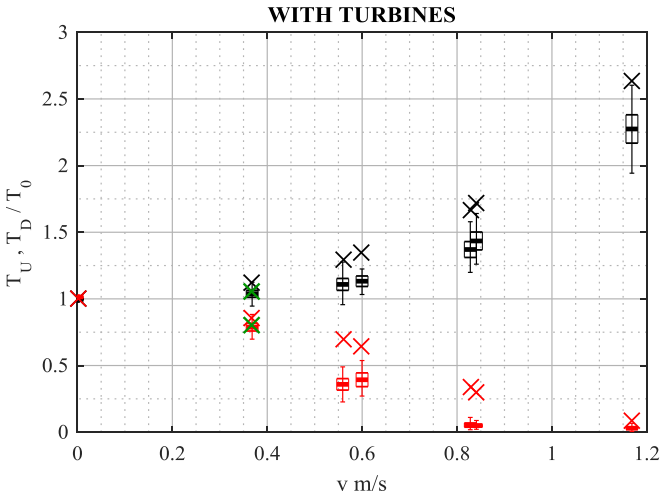

Fig. 17 Platform with turbines – mooring tensions validation

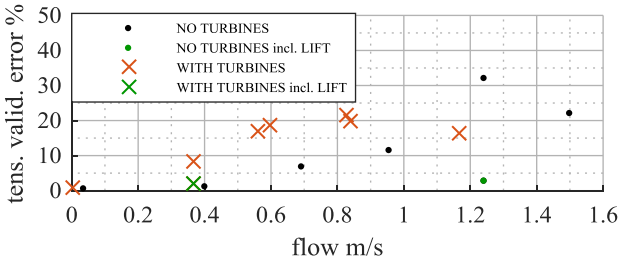

Fig. 15 Upstream line tension error (model – tank)

IV. DISCUSSION

The tank testing campaign provided valuable information on the response of PLAT-O #2 to axial currents in terms of motion and mooring tensions that proved the concept, validated modelling tools, identified areas of more in-depth studies and aided further design optimization. Given that all platform loads react in the moorings, the line tensions and vectors data allowed derivation of experimental drag and lift curves of the platform assembly for improved understanding of device behaviour and numerical model validation.

A squatting motion of the platform with turbines is observed in axial flows higher than 3.5 m/s at full-scale. The device position follows an arc motion about the loci of the upstream lines; as it surges with the flow, it gradually descends to a stable depth, maintaining tensions in the upstream lines and leaving the downstream lines slack. Consequently, the upstream mooring – bed angle (β_U, Fig. 4) is reduced, to balance tension components against vertical (Z) and horizontal (X) platform loads. The equilibrium of forces in the X-axis concerns the horizontal components of the upstream line tensions, platform drag (and thrust with turbines). The equilibrium of forces in the Z-axis concerns the vertical components of the upstream line tensions, platform net buoyancy and lift (Fig. 4).

In the previous study [4], lift was not modelled, and platform drag was over predicted (upper-bound curve in Fig. 10) to drive the squatting in the numerical model, resulting in a 30+% overestimation in upstream line tensions. A significant negative lift, and a significant drag reduction due to the Reynolds-regime approaching critical in the higher flows, were suspected in [4]. In this study, derivation of experimental drag and lift curves for the platform confirms the presence of a strong lift force and of Reynolds-dependent drag.

The platform with turbines experiences a significant lift, of up to 0.45 the pre-tension of a primary line, towards the bed, when pitching bow-up in axial flows (Fig. 11). Without the turbines and the thrust moment, the platform pitches bow-down and also experiences a downward lift.

The downward lift force acts against net buoyancy to lower line tensions. This is best seen in the 1.2 m/s test without turbines, where the tank upstream loads dip (Fig. 14) because the platform squats, pitches bow-down -4° and is subjected to the highest recorded lift of -0.7 (normalised against pre-tension) (Fig. 11). The downward lift encourages the squatting motion.

The main lift contributors are suspected to be the pair of lower beams of near-elliptical cross-section arranged in tandem. The lift acts sharply at the slightest pitch (or very low angles of attack) as seen in Figures 11 and 12. The negative lift comes into effect as soon the downstream lower beams are exposed to the flow causing complex interactions. Another source of lift could be the hydrofoil beams, which, although designed to stay level with flow, are following the pitch of the platform due to some resistance in the revolute joints. No measurement was made of the hydrofoil angle of attack.

The tested flow regime across the platform approaches critical as flow speeds increase. The tank-derived platform drag coefficient decreases with the Reynolds regime (refer to Fig. 9), by up to 15% at 1.2 m/s ($Re \approx 2\times10^5$), relative to the sub-critical at 0.4 m/s ($Re \approx 6\times10^4$).

Including the lift force and Reynolds-dependent drag in the numerical model improves agreement in tensions and motion. The modelling error in the upstream line tensions at 1.24 m/s without turbines, is reduced from 32% to 3% (Fig. 15) and the squatting is captured within one standard deviation (Fig. 13). In the rest of the flows cases without turbines, the lift is not accounted in the model and the squatting is underestimated and outside the measured range.

As a preliminary validation, lift is included and the thrust coefficient is calibrated (90% of the ideal value) in the 0.35 m/s test without turbines, to improve tension agreement from 8% to 2% (Fig. 15). In the rest of the flow cases, the tensions are overestimated by up to 20%, since the Reynolds-drag, the lift and the thrust calibration have not been incorporated in the numerical analysis for these loads cases.

From a mooring design perspective, the mooring geometry can be optimised to control the platform lift and the extent of squatting. Firstly, the mooring spread can be optimised such that the centre of effort better matches the load centres of drag and thrust to minimize platform pitch and therefore lift. Secondly, the mooring – bed angle can be reduced (i.e. a wider spread) to minimize the downward components of drag and thrust, and therefore the extent of squatting.

The platform acts as a hydrofoil of a complex profile in fast and turbulent flows. The turbines would likely have an impact on the resulting flow patterns around the platform. Further analysis is needed to pinpoint the platform drag and lift centres in relation to the mooring centre of effort. Dedicated platform experiments for lift and drag, similar to foils, can help to understand the complex lift force and where it acts depending on inflow, pitch angle and turbulence. A CFD analysis of drag and lift past the pair of lower beams is recommended (first), which could be extended to the rest of the platform to improve understanding of lift in the tank (near-critical regime) and the sea (post-critical regime). If the lower beams are found to be the main source of lift, these can be perforated or a truss structure can be implemented to limit lift.

The next stages in ProteusDS modelling are: completing the iteration with lift, Reynolds-dependent drag and thrust calibration for the remaining flow cases; incorporating flow turbulence; and expanding the validation to waves and current. At FloWave, the device was also tested in combined waves and currents [3]. The waves add another layer of complexity in terms of wave – current interaction, the impact of oscillatory flow on the development of lift, the impact of the *KC* number (besides *Re*) on the hydrodynamic parameters (*Cd* and *Cm*). The ProteusDS models will aid mooring design and specifications (load ratings and fatigue lifetimes) for various tidal climates (e.g. currents, waves, tidal range) and site constraints (e.g. bathymetry, array spacing).

V. Conclusion

The PLAT-O #2 concept is a floating subsea platform that supports four tidal turbines and is moored in tension by a bridled system with four anchors. A 1:17 scale physical model of this device was tested at FloWave in steady axial currents, with and without turbines. The motion and mooring tensions of the device were recorded to compare against a tank-scale numerical model in ProteusDS.

The device is experiencing complex lift forces that affect device motion and line tensions. In flows above 3.5 m/s at full-scale, the platform squats as it moves in an arc path along the upstream lines and about their anchors to a stable lower depth, whilst releasing tension in the downstream lines.

The platform lift characteristics are experimentally derived to indicate a significant force in the negative direction (towards the bed) when the platform (with turbines) pitches bow-up to the flow. The downward lift acts to lower line tensions but encourages the squatting motion.

The tested flow regime across the platform approaches critical in the higher flows. The tank-derived platform drag coefficient decreases with the Reynolds regime, by up to 15% at 1.2 m/s, relative to the sub-critical *Re* at 0.4 m/s.

Including the lift force, representing Reynolds-dependent drag effects and using a calibrated thrust value in the numerical model improves validation (from 30% to within 5%) comparing to the previous iteration and study [4].

A more in-depth understanding of platform drag and lift is needed to locate load centres and optimize mooring spread. Dedicated flume-testing of the platform for drag and lift, as performed for hydrofoils, is advised to locate the centres of lift and drag as a function of flow and pitch. The scaled experiments would help validate a CFD model, which would then be used to predict lift in conditions expected at sea.

Acknowledgment

The Author would like to extend his gratitude to the rest of the Authors for their valuable guidance, technical insights and motivation throughout. The Author would also like to thank:

1) the IDCORE team and Sponsors - Energy Technologies Institute (ETI) and Engineering and Physical Sciences Research Council (EPSRC) funding EP/J500847/1;
2) the Sustainable Marine Energy team for initiating, supervising and part-funding this research;
3) the FloWave team for support with tank testing;
4) the Dynamic Systems Analysis team for support with ProteusDS.

References

[1] Sustainable Marine Energy Ltd website. [Online]. Available at: http://sustainablemarine.com/

[2] SCHOTTEL SIT INSTREAM TURBINE. [Online]. Available at: https://www.schottel.de/schottel-hydro/sit-instream-turbine/

[3] P. Jeffcoate, F. Fiore, E. O'Farrell, R. Starzmann, S. Bischof "Comparison of Simulations of Taut-Moored Platform PLAT-O using ProteusDS with Experiments", in *Proc. AWTEC*, 2016

[4] I. Bivol, P. Jeffcoate, L. Johanning, R. Nicoll "PLAT-O#2 at FloWave: A tank-scale validation of ProteusDS dynamic analysis tool for floating tidal", in Proc. *EWTEC*, 2017

[5] *DNVGL ST 0164 Tidal Turbines,* DNV GL Standard, 2015

[6] *DNVGL OS E301 Position Mooring,* DNV GL Offshore Standard, 2015

[7] *API RP 2SK Recommended Practice for Design and Analysis of Stationkeeping Systems for Floating Structures,* American Petroleum Institute Recommended Practice, 2005

[8] D. Ingram, R. Wallace, A. Robinson, I. Bryden (2014), "The design and commissioning of the first, circular, combined current and wave test basin", *OCEANS 2014* - TAIPEI. IEEE, New York. doi: 10.1109/OCEANS-TAIPEI.2014.6964577

[9] EMEC, The European Marine Energy Centre, Available at: http://www.emec.org.uk/

[10] DSA Dynamic Systems Analysis. *ProteusDS Manual* Available at: https://dsa-ltd.ca/

[11] A. Baron, D. Steinke, A. Turner, G. Trowse, R. Cheel, A. Hay, R. Karsten, T. Roc, T. Jeans. "Dynamic Analysis Validation of Floating ecoSpray Tidal Energy Test Platform", in *Proc. EWTEC, 2017*

[12] B. Buckham, F. Driscoll, M. Nahon, "Development of a Finite Element Cable Model for Use in Low-Tension Dynamics Simulation", *Journal of Applied Mechanics*, Vol.71, July 2004

[13] D. Noble, T. Davey, T. Bruce, H. Smith, P. Kaklis, A. Robinson, "Spatial Variation of Currents Generated in the FloWave Ocean Energy Research Facility", in *Proc. EWTEC,* 2015

[14] *DNV RP C205 Environmental Conditions and Environmental Loads,* DNV Recommended Practice, 2014

[15] S. Chakrabarti, *Hydrodynamics of Offshore Structures,* WIT Press, 1987

[16] O. M. Faltinsen, *Sea loads on ships and offshore structures*, Cambridge University Press, 1990

[17] S. Hoerner, *Fluid-Dynamic Drag: Theoretical, Experimental and Statistical Information*, Published by the Author, 1965

[18] ESDU 84015, *Cylinder groups: mean forces on pairs of long circular cylinders*, IHS Global, 2012